ACS OMEGA

Open Access

http://pubs.acs.org/journal/acsodf

Article

Density Functional Theory Study of Cu_6 Nanoclusters as a Phenylalanine Detector

Ashok Singh Bahota, Keshav Kumar Singh, Arti Yadav, Rajni Chaudhary, Neelam Agrawal, and Poonam Tandon*

Cite This: *ACS Omega* 2024, 9, 276−282

Read Online

ACCESS | Metrics & More | Article Recommendations | Supporting Information

ABSTRACT: Research on amino acids is an attractive area because of their application in metabolism, cancer treatment, growth, and repair of body tissue, and RNA and DNA syntheses. Twenty amino acids are primarily responsible for protein synthesis. In our study, we used a Cu_6 nanocluster as an amino acid detector. For the investigation, we adsorbed amino acids on the Cu_6 nanocluster and studied their UV−visible spectra. It is observed that all of the Cu_6−amino acid complexes have peaks at near 380 nm wavelength except the Cu−phenylalanine complex, where two UV−visible peaks are found at wavelengths 351 nm (excitation energy 3.49 eV) and 403 nm (excitation energy 3.02 eV), respectively, which originated from the HOMO − 2 to LUMO (28%) and HOMO − 1 to LUMO (38%) transitions. Due to this unique transition, the Cu_6 nanocluster can be used for the detection of the phenylalanine amino acid out of the 20 amino acids.

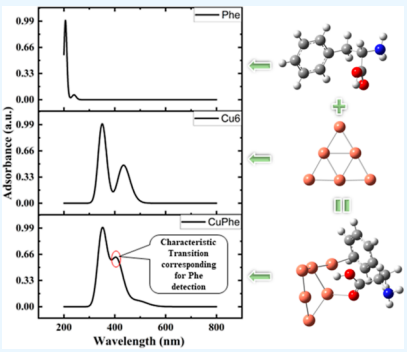

1. INTRODUCTION

Protein, one of three important macronutrients, is an important energy source for the human body. Proteins have two parts, short peptides and amino acids, and they can be adsorbed and digested in both forms (amino acid and peptides), and both have important physiological effects.[1−3] Amino acids present in the human plasma are in μM level concentrations.[4] They are not only regulators of gene expression but also neurotransmitters and precursors of several hormones. Amino acids play an important role as an intermediate in biosynthetic pathways.[1,5−7] Amino acids can be used for many other functions, for example, inhibitors (dehydroproline), neurotransmitters (gamma-aminobutyric acid), osmoregulation (proline), and metabolic intermediates (ornithine and citrulline).[8] Amino acids and their chemical analogues are used in the medical field, cosmetics, and in the synthesis of pharmaceutical agents. The synthetic polymer of amino acids is used as encapsulation in drugs and medicine because they are easily dissolved in water and can easily achieve controlled release in the bloodstream.[9] Branched-chain amino acids, valine, leucine, and isoleucine, are adsorbed in tumors besides tryptophan and arginine. Therefore, these amino acids and their complexes with other amino acids can be applied for the treatment of tumors, such as glycine being used for the biosynthesis of many nonprotein compounds (porphyrins and purines).[10] The role of amino acids is not limited to the nervous system but also their application in the biosynthesis of many essential compounds. The role of glutamine, aspartic, and glycine is not a limitation to the nervous system but also their application in the biosynthesis of many essential compounds (melanin, pyrimidine nucleotides, purine creatine, histamine, heme, and thyroxine).[7]

In recent years, metal nanoclusters have been a very attractive research field owing to their unique optical and physical properties. Metal nanoclusters have a diameter of 2 nm and a metal core has ten to hundred metal atoms.[11] Copper metal nanoclusters have unique chemical and physical characteristics with various applications in therapeutics and medical diagnostics, nanodevices, chemical sensors, catalysis, and many other fields.[12−14] Many research groups have researched metal nanoclusters as a detector,[15−24] some of which are briefly described here. Wang et al.[24] worked on the development of a sensor for the detection of glutathione with the help of MnO_2 nanosheet-copper nanocluster composites. This sensor may be useful for the detection of the glutathione levels in human sera. This sensor is low cost, has low cytotoxicity, has a turn-on fluorescence response, and is easy to develop. Guo and Cai[23] synthesized a water-soluble fluorescence ascorbic acid copper nanocluster, which is stable and well monodispersed with strong fluorescence. The fluorescence properties of these complexes can be quenched with the help of tetracycline. They found two linear relationships between F0 and F and tetracycline concen-

Received: July 18, 2023
Accepted: September 14, 2023
Published: December 21, 2023

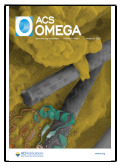

https://doi.org/10.1021/acsomega.3c04820
ACS Omega 2024, 9, 276−282

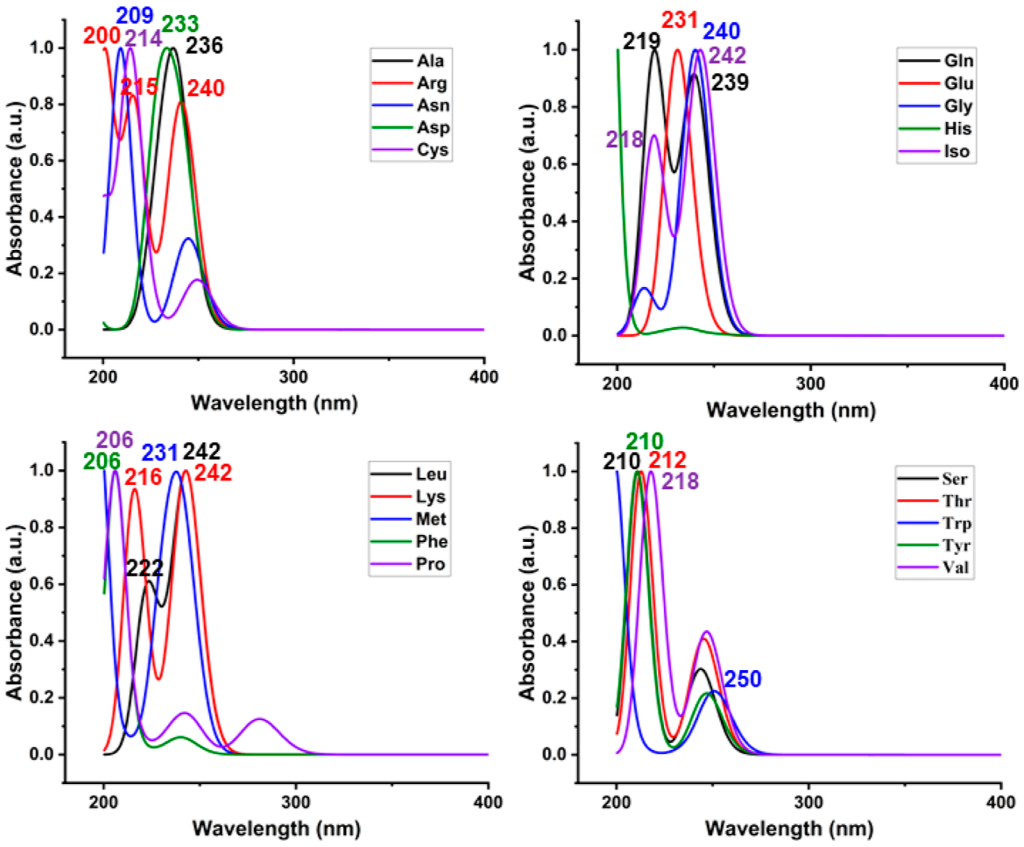

Figure 1. UV−visible spectra of amino acids calculated at the Cam-B3LPY/LanL2dz level of theory.

trations. These properties are more important in developing a detector for detecting tetracycline in environmental water with the help of fluorescence ascorbic acid copper nanoclusters. Gao and Cai[23] developed a sensor for the sensitive and selective detection of kojic acid in foodstuffs. This is a new, rapid, label-free, highly selective, and sensitive method. This process can work directly in aqueous solution. Its design is simple. This method is more accurate because of the interaction between the kojic acid and copper ions. Therefore, it is easier to apply in real samples. They say that this sensor can be applied for the monitoring and regulation of food safety and quality. Hu et al.[19] proposed a detector for H_2O_2 and glucose detection by copper nanoclusters. They investigated that the copper nanoclusters have intrinsic peroxidase-like activity. On finding these properties, they developed a simple and elective colorimetric detector, which can detect H_2O_2 and glucose. This work is useful in catalysis, medical diagnostics, and biotechnology. From the above discussion, it is clear that the interaction of metal nanoclusters with organic systems is significant for various applications. However, to the best of the author's knowledge, no research group has studied all complexes of all 20 proteinaceous amino acids with metal nanoclusters for the detection of amino acids. As such, in this work, we have studied complexes of Cu_6 metal nanoclusters and amino acids using the time-dependent density functional theory. The electronic spectra calculated via this method can provide a unique spectral signature, which will be helpful in detecting certain amino acids by observing their UV−vis spectra.

2. COMPUTATIONAL DETAILS

In this paper, we have chosen the Cu_6 metal nanocluster, which is the smallest stable copper metal nanocluster, as reported by Cui-Ju.[25] This reported structure and amino acid structures were optimized by Gaussian16.[26] In the case of metal nanoclusters, many research groups had worked with Møller−Plesset correlation energy corrections, which is more accurate than the other methods.[27−29] Therefore, we have chosen the MP2 method with a LanL2dz basis set to perform all optimization of Cu_6−amino acid complexes. It is reported that MP2/LanL2dz provides theoretically accurate energies. An analytical frequency calculation was performed after optimization, and all calculated frequencies were positive. Therefore, all the reported structures are true minima. However, this level of theory does not apply to performing time-dependent self-consistent field (TD-SCF) calculations. Therefore, time-dependent density functional theory (TD-DFT)[30] calculations were performed on MP2/LanL2dz optimized structures, using Cam-B3LPY/LanL2dz to calculate the electronic adsorption spectra of Cu_6 nanoclusters, and amino acids adsorbed on the Cu_6 nanocluster structure. In all TD-DFT calculations, 20 transition modes have been used.[11]

3. RESULTS AND DISCUSSION

3.1. UV−Visible Analysis. There is a large panel of understanding the time-dependent theory with the help of quantum chemistry of atoms, molecules, and complexes. In 1968, Song et al., on the basis of Pariser−Parr−Pople and Huckel methods, investigated the molecular orbital analysis and reported the electronic structures and spectra of anthocyanidins.[31] While in 1998, Pereira et al. worked on

https://doi.org/10.1021/acsomega.3c04820
ACS Omega 2024, 9, 276−282

Table 1. Excitation Energy, Theoretical Peak at Wavelength, Oscillator Strength, Major Contribution, and Experimental Literature Peaks at a Wavelength of Transition Orbital for the Cu_6 Nanocluster Adsorbed Amino Acid Complexes[a]

amino acids	theoretical peak at wavelength (nm)	excitation energy (eV)	oscillator strength	major contribution	experimental literature observed peaks at wavelength (nm)
Ala	236	5.03	0.0037	H − 1 → L (59%) H → L (40%)	240[36]
Arg	200	5.99	0.004	H − 2 → L + 1 (88%)	
	215	5.56	0.0033	H − 1 → L (69%)	
	240	4.99	0.0033	H − 4 → L (69%)	235[37]
Asn	209	5.74	0.0109	H → L (67%)	119[38]
Asp	233	5.25	0.0053	H → L (45%)	196 and 227[38]
Cys	214	5.61	0.0022	H → L (78%)	214[39]
Gln	219	5.48	0.0037	H → L (77%)	203 and 227[38]
	239	5.02	0.0027	H − 3 → L (72%)	
Glu	231	5.22	0.008	H → L (80%)	not found
Gly	240	5.00	0.0006	H − 1 → L (65%)	230[40]
His	198	6.20	0.2319	H → L + 1 (91%)	210[41]
Iso	218	5.49	0.0021	H → L (67%)	not found
	242	4.95	0.003	H − 1 → L (62%)	
Leu	222	5.39	0.0015	H → L (55%)	not found
	242	4.95	0.0025	H − 1 → L (54%) ,H → L (44%)	
Lys	216	5.56	0.0029	H − 1 → L (65%)	205[42]
	242	4.95	0.0031	H − 2 → L (61%)	
Met	231	4.99	0.0093	H − 1 → L (40%)	220[43]
Phe	206	5.83	0.0516	H → L + 1 (45%)	209[41]
Pro	206	5.83	0.0191	H → L + 3 (94%)	206[44]
Ser	210	5.70	0.0076	H − 2 → L (38%)	210[45]
	243	4.93	0.0023	H − 2 → L (59%)	
Thr	212	5.65	0.0066	H → L (59%)	202[46]
	245	4.90	0.0027	H − 2 → L (57%)	
Trp	250	4.82	0.081	H → L (33%)	260[36]
Tyr	210	5.70	0.1315	H → L + 2 (70%)	220[41]
	246	4.86	0.026	H → L (62%)	
Val	218	5.51	0.0092	H → L (59%)	203[47]
	246	4.87	0.004	H − 1 → L (57%)	

[a]Here represent HOMO by (H) and LUMO by (L).

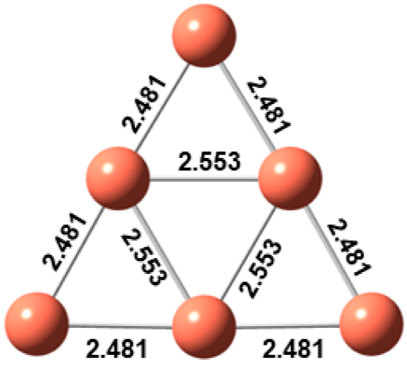

Figure 2. Optimized structure of the Cu_6 nanocluster.

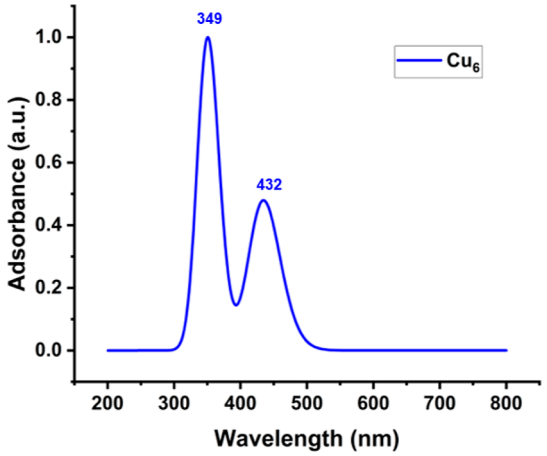

Figure 3. UV−visible spectra of the Cu_6 nanocluster.

the excited states of anthocyanidins with the density functional theory based on the single excitation−configuration interaction.[32] Sakata et al. worked on the anthocyanidin cationic molecules to evaluate UV/vis adsorption with time-dependent analysis.[33] Perpète et al. worked on the UV−vis analysis of a series of polyphenol derivatives and investigated that the Hartree−Fock and semiempirical approach does not give the approaching result as the experimental literature.[34] Freitas et al. used TD-DFT to investigate the optical properties of the flavylium cations. In recent years, TD-DFT has been an appropriate tool for understanding the UV−vis for small/large compounds, molecules, and atoms.[35]

In this article, all of the reported structures were optimized by the MP2/LanL2dz level of theory. TD-DFT calculations were performed to understand the UV−visible nature of Cu_6,

https://doi.org/10.1021/acsomega.3c04820
ACS Omega 2024, 9, 276−282

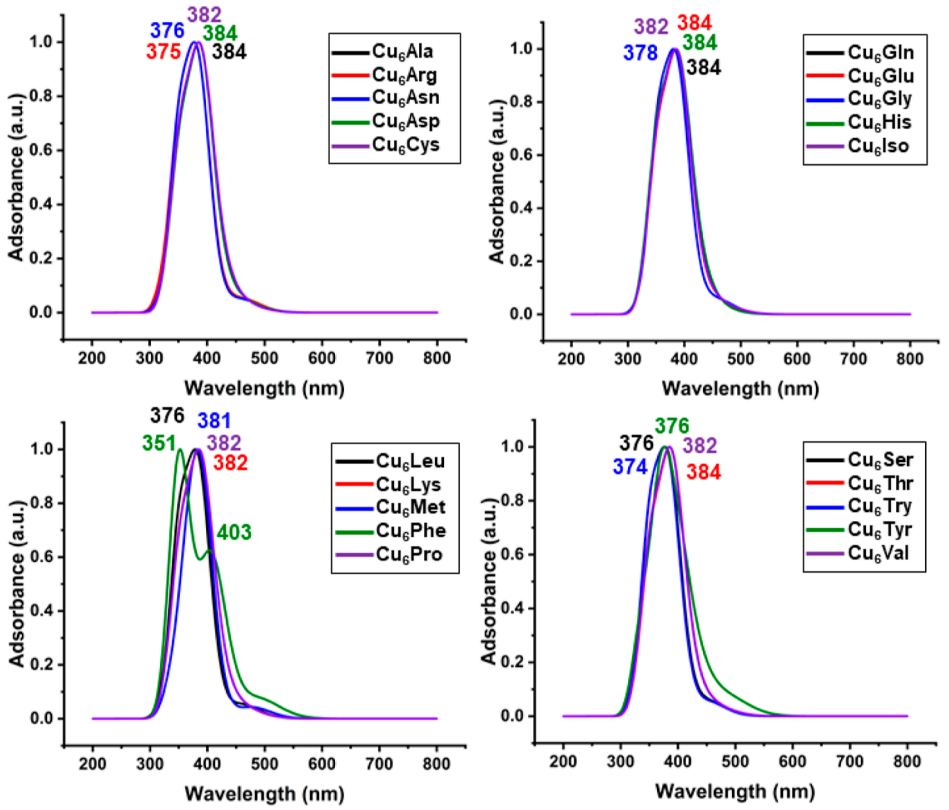

Figure 4. UV−visible spectra of Cu_6-adsorbed amino acid complexes.

amino acids, and Cu_6-adsorbed amino acids. All transitions were observed due to the presence of Cu_6 nanoclusters in all of the Cu_6-adsorbed amino acids. In the copper atom, transitions are possible in the d-orbital. Therefore, the molecular orbital transition possibility is only from the d orbital. There are only five orbitals (d_{xy}, d_{yx}, d_{zx}, $d_{x^2-y^2}$, and d_{z^2}) present in the d-orbital. Out of which, three orbits are nonbonding orbitals (d_{xy}, d_{yx}, and d_{zx}) and the other two ($d_{x^2-y^2}$ and d_{z^2}) present both bonding orbitals and their antibonding orbitals.

We first studied the UV−visible spectra obtained from the TD-DFT calculation of the amino acids in order to compare the UV excitation wavelengths before and after adsorption on Cu_6. The UV−visible plots of the amino acids are shown in Figure 1 and the excitation energy, oscillator strength, peaks, and major contribution are reported in Table 1. In Figure 1, it is observed that in all the amino acids, UV−visible peaks are observed between the 200 and 250 nm wavelength range. Detailed results from these calculations and their comparison with previously reported experimental literature are listed in Table 1. In Table 1, a maximum of a ±10−15 nm difference is observed between excitation peaks calculated by us and the experimental ones reported in the literature. Therefore, we can say that the method which has been chosen for the UV−visible calculation provides results that are close to the experimental literature. Therefore, this theoretical method is a more suitable method to understand the UV−visible properties of the amino acid and Cu-adsorbed amino acid. In most of the amino acids (Ala, Asn, Asp, Cys, Gln, Glu, Leu, Thr, Trp, Try, and Val), the transition has occurred due to the HOMO (H) to LUMO (L) transition. While in the Ala, Arg, Gly, Iso, Leu, Lys, Met, and Val amino acids, the transition has been found due to the transition of H − 1 to L. In the remaining amino acids, the transition occurs due to different molecular orbitals. The excitation energy of most of the amino acids has been observed between the range of 4.81−6.02 eV. While the oscillator strength is below 0.2319 in the amino acids. In contrast to previously reported (experimental literature) UV spectra, in our theoretical work, some additional small peaks were also observed in the UV−visible spectrum of almost all amino acids. However, these additional peaks have low oscillator strength in comparison to the most intense peak. Therefore, these additional peaks were not observed in experimental literature spectra.

To study adsorption of amino acids on Cu_6 nanoclusters, we first took its initial structure from ref 25 and optimized that Cu_6 nanocluster at the MP2/LanL2dz level of theory to maintain consistency throughout our work. This optimized structure is shown in Figure 2. In the Cu_6 nanoclusters, the bond length of all six outer bonds is 2.48 Å, and the inner three bonds are 2.55 Å. It (Cu_6 nanocluster) has a D_{3h} point group symmetry. To find suitable positions to adsorb amino acids on this nanocluster, we consider the Mulliken charge of the Cu_6 nanocluster and the amino acids. We observed that the Cu_6 nanocluster has the same positive charge (0.25e) at each corner, while amino acids have a more negative charge (range from −0.26 to −0.30e) at the O of the −C═O group of the −COOH moiety. Therefore, they can easily interact with each other due to the electrostatic interaction. Thus, we interact with them on that side. The oxygen atom of the −C═O group of the −COOH moiety of amino acids was kept at 2.92 Å (sum of Vander Wall radius), as shown in Figure S1. All of the structures obtained after optimization of these input structures are reported in Figure S2. In Figure S2, it is clear that the average bond length between Cu−O decreases and becomes 2.46 to 2.55 Å in the optimized Cu_6−amino acid complexes. While in the Cu_6Phe and Cu_6Tyr complexes, the Cu atoms of

https://doi.org/10.1021/acsomega.3c04820
ACS Omega 2024, 9, 276−282

Table 2. Excitation Energy, Wavelength, Oscillator Strength, and Major Contribution of Transition Orbital for Cu_6 Nanoclusters and Cu_6 Nanocluster Adsorbed Amino Acid Complexes (Cu_6–Amino Acids)[a]

complex	wavelength (nm)	excitation energy (eV)	oscillator strength	major contribution
Cu_6	349	3.50	0.1992	H − 4 → L (36%)
	432	2.86	0.1648	H − 1 → L (85%)
Cu_6Ala	384	3.19	0.4572	H − 1 → L + 1 (39%)
Cu_6Arg	375	3.23	0.3821	H − 1 → L (23%)
Cu_6Asn	376	3.22	0.5059	H − 1 → L (45%)
Cu_6Asp	384	3.19	0.463	H − 1 → L + 1 (38%)
Cu_6Cys	382	3.19	0.4436	H − 1 → L + 1 (42%)
Cu_6Gln	384	3.19	0.4422	H − 1 → L + 1 (40%)
Cu_6Glu	384	3.19	0.4603	H − 1 → L + 1 (35%)
Cu_6Gly	378	3.18	0.4385	H − 1 → L (38%)
Cu_6His	384	3.18	0.4278	H − 1 → L + 1 (45%)
Cu_6Iso	382	3.19	0.454	H − 1 → L + 1 (40%)
Cu_6Leu	376	3.21	0.5224	H − 1 → L (45%)
Cu_6Lys	382	3.19	0.4533	H − 1 → L + 1 (40%)
Cu_6Met	381	3.17	0.5476	H − 1 → L (59%)
Cu_6Phe	351	3.49	0.1755	H − 2 → L (28%)
	403	3.02	0.2108	H − 1 → L (38%)
Cu_6Pro	382	3.19	0.4527	H − 1 → L + 1 (40%)
Cu_6Ser	376	3.20	0.469	H − 1 → L (44%)
Cu_6Thr	384	3.19	0.4578	H − 1 → L + 1 (39%)
Cu_6Try	374	3.22	0.4837	H − 1 → L (40%)
Cu_6Tyr	376	3.32	0.2293	H − 1 → L + 2 (49%)
Cu_6Val	382	3.19	0.4556	H − 1 → L + 1 (39%)

[a]Here represent HOMO by (H) and LUMO by (L).

the Cu_6 nanocluster also interact with the carbon atom of the ring fragment of Phe and Tyr amino acids. Due to this interaction, the bond lengths between Cu−O are 2.20 and 2.16 Å in the Cu_6Phe and Cu_6Tyr complexes, respectively. While the bond lengths between Cu−C are 2.34 and 2.41 Å in the Cu_6Phe and Cu_6Tyr complexes, respectively. Similarly, the bond length between Cu−Cu atoms has been observed to range from 2.05 to 2.10 Å in the Cu_6 nanoclusters of Cu_6–amino acid complexes. We analyzed the TD-DFT properties after the optimization of these complexes. UV−visible spectra for the Cu_6 nanocluster and Cu_6-adsorbed amino acids are shown in Figures 3 and 4.

In Figure 3, 4 and Table 2, it is clear that the UV−vis peak of Cu_6 nanocluster has been found at 349 and 432 nm with excitation energies of 3.50 and 2.86 eV, respectively. The oscillator strength for the 432 nm peaks is 0.1648 and the 349 nm peak is 0.1992 in the Cu_6 nanocluster. A peak of 349 nm arises due to the H − 4 → L (36%) transition. While the peak at 432 nm is due to the H − 1 → L (85%) transition. Similarly, in all the Cu amino acid complexes, the UV−visible transition peaks observed a range from 374 to 384 nm wavelength except the Cu_6Phe complex. In this complex (Cu_6Phe), two transition peaks were observed at 349 and 403 nm wavelengths. While

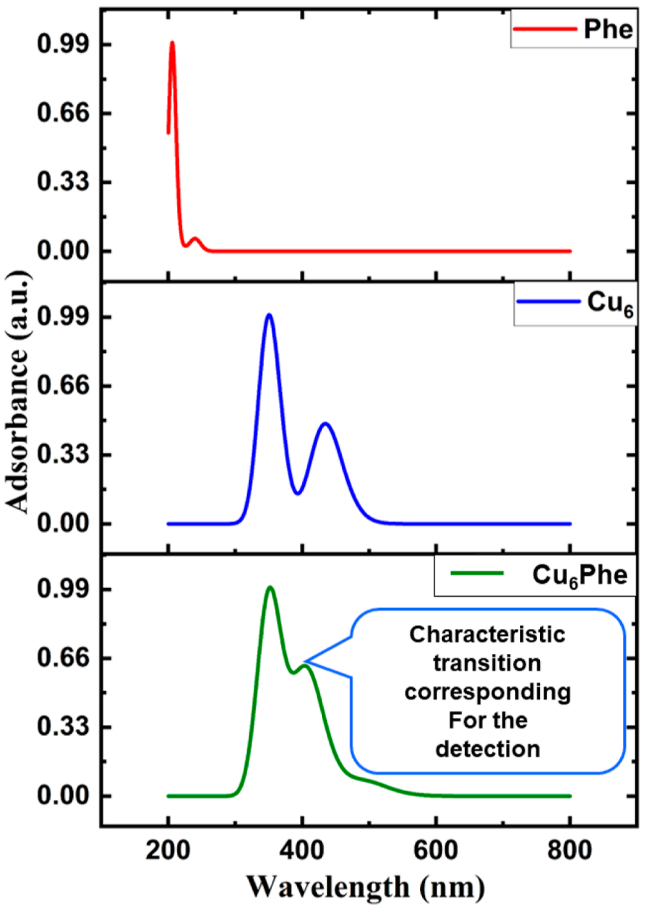

Figure 5. UV−visible spectra of the Cu_6, Phe, and Cu_6Phe complexes to understand the characteristic transition corresponding to Phe detection.

the excitation energy of most of the complexes (except the Cu_6Phe complex) was observed in the range from 3.19 to 3.32 eV and the oscillator strength of these complexes ranged from 0.293 to 0.5059. The transition occurred in the Cu_6Arg, Cu_6Asn, Cu_6Gly, Cu_6Leu, Cu_6Met, Cu_6Phe, Cu_6Ser, and Cu_6Try complexes due to the transition from HOMO − 1 to LUMO. While in the Cu_6Ala, Cu_6Asp, Cu_6Cys, Cu_6Gln, Cu_6Glu, Cu_6His, Cu_6Iso, Cu_6Lys, Cu_6Pro, Cu_6Thr, and Cu_6Val complexes, the transition occurs from HOMO − 1 to LUMO + 1. Only in the Cu_6Tyr complex, the transition occurred due to the transition from HOMO − 1 to LUMO + 2. In all the Cu_6-adsorbed amino acid complexes, except the Cu_6Phe complex, most of the complexes have one transition peak in UV−visible spectra.

When Phe and Tyr amino acids interact with the Cu_6 nanocluster, then the Cu_6 nanocluster interacts with two sides of Phe and Tyr amino acids, as shown in Figure S1. While the interaction between Cu and Phe amino is stronger than the Cu_6Tyr complex. The bond lengths between Cu−C are 2.34 and 2.41 Å in the Cu_6Phe and Cu_6Tyr complexes, respectively. Therefore, it is clear that the interaction between Cu and C in the Phe complex is stronger in comparison to the Cu_6Tyr complex. Therefore, in the Cu_6Phe complex, Cu_6 breaks from its initial structure and changes to a different type of structure. Due to this effect, internal bonding is affected. Therefore, in UV−visible spectra, Cu_6Phe complexes have two peaks. These two peaks occurred due to the two transitions from the Cu_6 nanocluster with different HOMO and LUMO orbitals. Out of

https://doi.org/10.1021/acsomega.3c04820
ACS Omega 2024, 9, 276−282

these transitions, one transition occurred due to the transition of H − 2 → L (28%), and another transition from the H − 1 → L (38%) transition. Due to these two transitions, two different peaks were observed at 351 and 403 nm wavelengths, with oscillator strengths being 0.1755 and 0.2108, respectively. The excitation energies of these peaks are observed at 3.49 and 3.02 eV, respectively. These excitation energies were the highest and lowest excitation energies in comparison to those of the other complexes.

When the Cu_6 nanocluster interacts with amino acids and forms complexes, the UV−visible peaks are observed in the range from 374 to 384 nm wavelength. Therefore, in a sample containing a mixture of multiple amino acids, if we use Cu_6 as a detector, we will observe all the merged peaks ranging from 374 to 384 nm wavelength. No information can be obtained from this type of spectrum because it will be difficult to identify, which peak belongs to which amino acid. However, a peak at 403 nm can be uniquely identified in such a scenario. This peak belongs to the Cu_6Phe complex. This complex also has another peak at 351 nm. A comparison between the excitation wavelengths of the Phe amino acid, Cu_6 nanocluster, and Cu_6Phe complex is shown in Figure 5. In Figure 5, it is clear that the peaks at 349 nm (Cu_6 nanoclusters) and 351 nm (Cu_6Phe complex) will be merged and cannot be identified. While in the Cu_6Phe complex, the peak at 403 nm can be uniquely observed. It has a suitable oscillator strength (0.2108) for observation in the experimental literature observation.

4. CONCLUSIONS

In this article, we selected the smallest stable Cu_6 nanocluster,[25] and we studied the interaction of this nanocluster with all amino acids. We performed ab initio calculations at the MP2/LanL2DZ theory level to understand the optimized structures. After the optimization, TD-DFT with 20 transitions was used to understand the UV−visible adsorption properties of these structures. From the UV−visible spectra, it is observed that two peaks are observed at 484 and 398 nm in the Cu_6 nanoclusters. While the peaks are observed between the range 200−250 nm in the amino acids. When studying interacting complexes, it is analyzed that most of the structure's peak is at the 380−390 nm range. While in the Cu_6Phe complex, we found the two peaks at 351 and 403 nm. The oscillator strength of these two peaks is 0.1755 and 0.2108, respectively, which are suitable for the experimental observation. Therefore, the Cu_6 nanocluster can be used as a Phe amino acid detector. The application of this work is to identify the Phe amino acid in a mixture of two or more amino acids. Phe and other amino acids are used in skin products, protein products, biotechnology, and medicine. Therefore, we can detect whether or not Phe is present in it or not.

■ ASSOCIATED CONTENT

Supporting Information

The Supporting Information is available free of charge at https://pubs.acs.org/doi/10.1021/acsomega.3c04820.

Input and optimized structures of Cu6- amino acid complexes with relevant bond lengths (PDF)

■ AUTHOR INFORMATION

Corresponding Author

Poonam Tandon − *Department of Physics, University of Lucknow, 226007 Lucknow, Uttar Pradesh, India;* orcid.org/0000-0002-8120-0498; Email: tandon_poonam@lkouniv.ac.in

Authors

Ashok Singh Bahota − *Department of Physics, University of Lucknow, 226007 Lucknow, Uttar Pradesh, India*

Keshav Kumar Singh − *Department of Physics, University of Lucknow, 226007 Lucknow, Uttar Pradesh, India*

Arti Yadav − *Department of Physics, University of Lucknow, 226007 Lucknow, Uttar Pradesh, India*

Rajni Chaudhary − *Department of Physics, University of Lucknow, 226007 Lucknow, Uttar Pradesh, India*

Neelam Agrawal − *Department of Physics, University of Lucknow, 226007 Lucknow, Uttar Pradesh, India*

Complete contact information is available at: https://pubs.acs.org/10.1021/acsomega.3c04820

Author Contributions

Ashok Singh Bahota: conceptualization, data curation, funding acquisition, formal analysis, investigation, methodology, validation, writing—original draft, and plotting figure-except UV−visible. **Keshav Kumar Singh:** conceptualization, writing−review and editing. **Arti Yadav:** methodology and introduction. **Rajni Chaudhary:** introduction, funding acquisition, and methodology. **Neelam Agrawal:** methodology. **Poonam Tandon:** resources, software, supervision, validation, and visualization.

Notes

The authors declare no competing financial interest.

■ ACKNOWLEDGMENTS

The financial support to A.S.B. from University Grants Commission ref. no. 1468/(SC)(CSIR-UGC NET DEC. 2016). R.C. from DST, India under DST-INSPIRE fellowship (2018/IF18021).

■ ABBREVIATIONS

Ala, alanine; Arg, arginine; Asn, asparagine; Asp, aspartic acid; Cys, cystine; Glu, glutamine; Glu, glutamic acid; Gly, glycine; His, histidine; Iso, isoleucine; Leu, leucine; Lys, lysine; Met, methionine; Phe, phenylalanine; Pro, proline; Ser, serine; Thr, threonine; Try, tryptophan; Tyr, tyrosine; Val, valine; UV−visible, ultraviolet−visible; HOMO, highest occupied molecular orbital; LUMO, lowest unoccupied molecular orbital; Cu_6, copper nanocluster of six atoms; Cu, copper

■ REFERENCES

(1) Rose, A. J. Amino acid nutrition and metabolism in health and disease. *Nutrients* **2019**, *11* (11), 2623.

(2) Iacone, R.; Scanzano, C.; Santarpia, L.; Cioffi, I.; Contaldo, F., Pasanisi, F., **2020**.

(3) Overduin, J.; Frayo, R. S.; Grill, H. J.; Kaplan, J. M.; Cummings, D. E. Role of the duodenum and macronutrient type in ghrelin regulation. *Endocrinology* **2005**, *146* (2), 845−850.

(4) Iacone, R.; et al. Macronutrients in parenteral nutrition: amino acids. *Nutrients* **2020**, *12* (3), 772.

(5) Ta, H. Y.; Collin, F.; Perquis, L.; Poinsot, V.; Ong-Meang, V.; Couderc, F. Twenty years of amino acid determination using capillary electrophoresis: A review. *Anal. Chim. Acta* **2021**, *1174*, 338233.

(6) Ferré, S.; González-Ruiz, V.; Guillarme, D.; Rudaz, S. Analytical strategies for the determination of amino acids: Past, present and future trends. *J. Chromatogr. B* **2019**, *1132*, 121819.

(7) Nussenzweig, V.; Sonntag, R., Biancalana, A. *Amino Acid Disorders*; Elsevier, 2003.

(8) Maloy, S. Amino acids. In *Brenner's Encyclopedia of Genetics*, 2nd ed.; Maloy, S.; Hughes, K., Eds.; Academic Press: San Diego, 2013; pp 108−110.
(9) Berg, J. M.; Tymoczko, J. L.; Stryer, L. *Biochemistry*, 5th ed.; W. H. Freeman Publishing: New York, 2002.
(10) Bhagavan, N. V., Ha, C.-E. *Amino acid Essentials of Medical Biochemistry*, 2nd ed.; Academic Press, 2015; pp 21−29.
(11) Bahota, A. S.; Singh, K. K.; Kumar, R.; Tandon, P. Ab-initio simulation of the interaction of gold nanoclusters with glycine. *J. Mol. Struct.* **2022**, *1266*, 133447.
(12) Liu, X.; Astruc, D. Atomically precise copper nanoclusters and their applications. *Coord. Chem. Rev.* **2018**, *359*, 112−126.
(13) Lin, Y. S.; Lin, Y. F.; Nain, A.; Huang, Y. F.; Chang, H. T. A critical review of copper nanoclusters for monitoring of water quality. *Sens. Actuators Rep.* **2021**, *3*, 100026.
(14) Lin, Y. S.; Chiu, T. C.; Hu, C. C. Fluorescence-tunable copper nanoclusters and their application in hexavalent chromium sensing. *RSC Adv.* **2019**, *9* (16), 9228−9234.
(15) Shang, L.; Dong, S. Silver nanocluster-based fluorescent sensors for sensitive detection of Cu (II). *J. Mater. Chem.* **2008**, *18* (39), 4636−4640.
(16) Chen, W. Y.; Lan, G. Y.; Chang, H. T. Use of fluorescent DNA-templated gold/silver nanoclusters for the detection of sulfide ions. *Anal. Chem.* **2011**, *83* (24), 9450−9455.
(17) Govindaraju, S.; Ankireddy, S. R.; Viswanath, B.; Kim, J.; Yun, K. Fluorescent gold nanoclusters for selective detection of dopamine in cerebrospinal fluid. *Sci. Rep.* **2017**, *7* (1), 40298.
(18) An, Y.; Ren, Y.; Bick, M.; Dudek, A.; Hong-Wang Waworuntu, E.; Tang, J.; Chen, J.; Chang, B. Highly fluorescent copper nanoclusters for sensing and bioimaging. *Biosens. Bioelectron.* **2020**, *154*, 112078.
(19) Hu, L.; Yuan, Y.; Zhang, L.; Zhao, J.; Majeed, S.; Xu, G. Copper nanoclusters as peroxidase mimetics and their applications to H2O2 and glucose detection. *Anal. Chim. Acta* **2013**, *762*, 83−86.
(20) Wang, X.; Long, C.; Jiang, Z.; Qing, T.; Zhang, K.; Zhang, P.; Feng, B. In situ synthesis of fluorescent copper nanoclusters for rapid detection of ascorbic acid in biological samples. *Anal. Methods* **2019**, *11* (36), 4580−4585.
(21) Lettieri, M.; Palladino, P.; Scarano, S.; Minunni, M. Copper nanoclusters and their application for innovative fluorescent detection strategies: An overview. *Sens. Actuators Rep.* **2022**, *4*, 100108.
(22) Gao, Z.; Su, R.; Qi, W.; Wang, L.; He, Z. Copper nanocluster-based fluorescent sensors for sensitive and selective detection of kojic acid in food stuff. *Sens. Actuators, B* **2014**, *195*, 359−364.
(23) Guo, Y.; Cai, Z. Ascorbic acid stabilized copper nanoclusters as fluorescent probes for selective detection of tetracycline. *Chem. Phys. Lett.* **2020**, *759*, 138048.
(24) Wang, H. B.; Chen, Y.; Li, Y.; Liu, Y. M. A sensitive fluorescence sensor for glutathione detection based on MnO 2 nanosheets−copper nanoclusters composites. *RSC Adv.* **2016**, *6* (83), 79526−79532.
(25) Cui-Ju, F.; Xiao-Yan, Z. Structures and Electronic Properties of CuN (N≤ 13) Clusters. *Commun. Theor. Phys.* **2009**, *52* (4), 675−680.
(26) Frisch, M. J.; Trucks, G. W.; Schlegel, H. B.; Scuseria, G. E.; Robb, M. A.; Cheeseman, J. R.; Scalmani, G.; Barone, V.; Petersson, G. A.; Nakatsuji, H. J. R. A.; Li, X. *Gaussian 16*, 2016.
(27) Pakiari, A. H.; Jamshidi, Z. Nature and strength of M- S Bonds (M= Au, Ag, and Cu) in binary alloy gold clusters. *J. Phys. Chem. A* **2010**, *114* (34), 9212−9221.
(28) Cramer, C. J.; Truhlar, D. G. Density functional theory for transition metals and transition metal chemistry. *Phys. Chem. Chem. Phys.* **2009**, *11* (46), 10757−10816.
(29) Jamshidi, Z.; Farhangian, H.; Tehrani, Z. A. Glucose interaction with Au, Ag, and Cu clusters: Theoretical investigation. *Int. J. Quantum Chem.* **2013**, *113* (8), 1062−1070.
(30) Marques, M. A.; Gross, E. K. Time-dependent density functional theory. *Annu. Rev. Phys. Chem.* **2004**, *55* (1), 427−455.
(31) Kurtin, W. E.; Song, P.-S. Electronic structures and spectra of some natural products of theoretical interest−I: Molecular orbital studies of anthocyanidins. *Tetrahedron* **1968**, *24* (5), 2255−2267.
(32) Pereira, G. K.; Galembeck, S. E. Computational study of the electronic excitations of some anthocyanidins. *Spectrochim. Acta, Part A* **1998**, *54* (2), 339−348.
(33) Sakata, K.; Saito, N.; Honda, T. Ab initio study of molecular structures and excited states in anthocyanidins. *Tetrahedron* **2006**, *62* (15), 3721−3731.
(34) Perpète, E. A.; Wathelet, V.; Preat, J.; Lambert, C.; Jacquemin, D. Toward a theoretical quantitative estimation of the λ_{max} of anthraquinones-based dyes. *J. Chem. Theory Comput.* **2006**, *2* (2), 434−440.
(35) Anouar, E. H.; Gierschner, J.; Duroux, J. L.; Trouillas, P. UV/Visible spectra of natural polyphenols: A time-dependent density functional theory study. *Food Chem.* **2012**, *131* (1), 79−89.
(36) Cavani, L.; Ciavatta, C.; Gessa, C. Determination of free L-and D-alanine in hydrolysed protein fertilisers by capillary electrophoresis. *J. Chromatogr. A* **2003**, *985* (1−2), 463−469.
(37) Ramya, K.; Raja, C. R. Studies on the growth and characterization of L-arginine maleate dihydrate crystal grown from liquid diffusion technique. *J. Miner. Mater. Charact. Eng.* **2016**, *04* (02), 143−153.
(38) Pang, X.; Zeng, H.; Liu, J.; Wei, S.; Zheng, Y. The properties of nanohydroxyapatite materials and its biological effects. *Mater. Sci. Appl.* **2010**, *01* (02), 81−90.
(39) Biçer, E.; Çetinkaya, P. A voltammetric study on the interaction of novobiocin with cysteine: pH effect. *J. Chil. Chem. Soc.* **2009**, *54* (1), 46−50.
(40) Chagas, M. A. S.; Galvão, A. D.; de Moraes, F. T.; Ribeiro, A. T. B. N.; de Siqueira, A. B.; de Assis Salama, I. C. C.; Arrais-Silva, W. W.; de Sousa, K. M. D.; de Sousa Pereira, C. C.; dos Santos, W. B. Synthesis, Characterization and Analysis of Leishmanicide Ability of the Compound [Ru (Cl) 3 (H2O) 2 (gly)]. *Open J. Inorg. Chem.* **2017**, *07* (04), 89−101.
(41) Wetlaufer, D. B. Ultraviolet spectra of proteins and amino acids. *Adv. Protein Chem.* **1963**, *17*, 303−390.
(42) Stagi, L.; Malfatti, L.; Caboi, F.; Innocenzi, P. Thermal Induced Polymerization of l-Lysine forms Branched Particles with Blue Fluorescence. *Macromol. Chem. Phys.* **2021**, *222* (20), 2100242.
(43) Angheluta, A.; Guizani, S.; Saunier, J.; Rönnback, R. Application of chemometric modelling to UV-Vis spectroscopy: development of simultaneous API and critical excipient assay in a liquid solution continuous flow. *Pharm. Dev. Technol.* **2020**, *25* (8), 919−929.
(44) Renuga, V. Synthesis, characterization and biological activity of pure and metal ions doped L-proline amino acid. *Int. J. Sci. Res.* **2014**, *4*, 170.
(45) Rajesh, K.; Kumar, P. P. Structural, linear, and nonlinear optical and mechanical properties of new organic L-Serine crystal. *Space* **2014**, *2014*, 790957.
(46) Ramesh Kumar, G.; Gokul Raj, S. Growth and physiochemical properties of second-order nonlinear optical L-threonine single crystals. *Adv. Mater. Sci. Eng.* **2009**, *2009*, 1−40.
(47) Malini, M. J.; Sangeetha, M. K.; Kunjitham, R.; Mariappan, M.; Ravindran, B.; Kamali, S. Effect of Cadmium sulphate on the Growth and Characterization of L Valine Crystal. *Int. J. Multidiscip.* **2018**, *3*, 319.

https://doi.org/10.1021/acsomega.3c04820
ACS Omega 2024, 9, 276−282